nature nanotechnology

LETTERS

PUBLISHED ONLINE: 4 DECEMBER 2011 | DOI: 10.1038/NNANO.2011.213

Solid-state memories based on ferroelectric tunnel junctions

André Chanthbouala[1], Arnaud Crassous[1], Vincent Garcia[1]*, Karim Bouzehouane[1], Stéphane Fusil[1,2], Xavier Moya[3], Julie Allibe[1], Bruno Dlubak[1], Julie Grollier[1], Stéphane Xavier[4], Cyrile Deranlot[1], Amir Moshar[5], Roger Proksch[5], Neil D. Mathur[3], Manuel Bibes[1] and Agnès Barthélémy[1]

Ferroic-order parameters[1] are useful as state variables in non-volatile information storage media because they show a hysteretic dependence on their electric or magnetic field. Coupling ferroics with quantum-mechanical tunnelling allows a simple and fast readout of the stored information through the influence of ferroic orders on the tunnel current. For example, data in magnetic random-access memories[2] are stored in the relative alignment of two ferromagnetic electrodes separated by a non-magnetic tunnel barrier, and data readout is accomplished by a tunnel current measurement. However, such devices based on tunnel magnetoresistance[3] typically exhibit OFF/ON ratios of less than 4, and require high powers for write operations (>1×10^6 A cm^{-2}). Here, we report non-volatile memories with OFF/ON ratios as high as 100 and write powers as low as $\sim 1 \times 10^4$ A cm^{-2} at room temperature by storing data in the electric polarization direction of a ferroelectric tunnel barrier. The junctions show large, stable, reproducible and reliable tunnel electroresistance, with resistance switching occurring at the coercive voltage of ferroelectric switching. These ferroelectric devices emerge as an alternative to other resistive memories[4], and have the advantage of not being based on voltage-induced migration of matter at the nanoscale[5,6], but on a purely electronic mechanism[7].

A ferroelectric tunnel junction (FTJ) is composed of a few-unit-cell ferroelectric thin film sandwiched between two electrodes. Applying an electric field across the ferroelectric film enables the reversal of its order parameter (the ferroelectric polarization), giving rise to two logic states with polarization pointing either up or down. Switching the ferroelectric polarization is predicted to give rise to large changes in the tunnel resistance, an effect called giant tunnel electroresistance (TER)[8]. TER can be produced by at least three mechanisms that depend on polarization direction[9]: (i) asymmetrical deformation of the barrier potential profile[10], (ii) changes in the density of states at the barrier/electrode interfaces and (iii) voltage-dependent variations of the barrier thickness due to piezoelectricity[11]. In 1971, Esaki *et al.* proposed the first concept for an FTJ, at that time termed a 'polar switch'[12]. However, because of the difficulty in preserving ferroelectricity down to thicknesses compatible with quantum-mechanical electron tunnelling[13–16], experiments with FTJs only began a few decades later. In 2003, one group reported TER at room temperature, without being able to clearly ascribe the resistive switching events to ferroelectric polarization reversal[17]. This group later pointed out the difficulty in distinguishing ferroelectricity-driven TER from resistive switching related to ionic displacements (such as electromigration)[18]. By combining piezoresponse force microscopy (PFM) and conductive-tip atomic force microscopy (CTAFM), several groups demonstrated conclusively in 2009 that switching ferroelectric domains in bare ferroelectric tunnel barriers leads to large TER at room temperature[19–21]. Here, we report the observation of giant TER at room temperature in solid-state ferroelectric tunnel junctions and qualify them as high-potential non-volatile random access memories. Although leakage current is detrimental in conventional capacitive ferroelectric random access memories (FeRAMs), these ferroelectric resistive memories take advantage of it to read information non-destructively[19].

The $BaTiO_3$(2 nm)/$La_{0.67}Sr_{0.33}MnO_3$(30 nm) (BTO/LSMO) heterostructures used in this study were grown on (001)$NdGaO_3$ single-crystal substrates by pulsed laser deposition (see Methods and ref. 19). The BTO film is fully strained, which favours the stabilization of a ferroelectric character at room temperature[22], as confirmed by PFM[19]. The PFM signal does not decay significantly over several days on these BTO ultrathin films, excluding other mechanisms related to ionic dynamics[23]. The BTO/LSMO bilayer was left unpatterned and gold(10 nm)/cobalt(10 nm) top-electrode circular pads (typically 500 nm in diameter) were defined by electron-beam lithography and lift-off (see Methods). An AFM image of four junctions and a sketch of their structure are presented in Fig. 1.

To measure the ferroelectric properties of the BTO barrier and the electrical response of the junctions, an electrical contact on the top-electrode pads was made using an AFM conductive tip. Figure 2a,b shows the results of PFM characterization for a representative junction. The out-of-plane piezoresponse acquired as a function of the d.c. voltage between the top and bottom electrodes shows a clear hysteretic behaviour, both in the phase (Fig. 2a) and amplitude (Fig. 2b) signals, suggesting a ferroelectric character for the BTO barrier integrated in the junctions. As expected for a ferroelectric signal, the phase difference between the two polarization states is $\sim 180^\circ$, and the minima in the amplitude loop coincide with the switching voltages in the phase signal. As bias voltage is applied to the cobalt electrode, these data suggest that applying a positive voltage orients the ferroelectric polarization towards the LSMO, whereas applying a negative voltage orients it towards the cobalt, with coercive voltages V_C of ~ 2 V (absolute value).

To investigate resistive switching in our ferroelectric devices, we applied short voltage pulses through the AFM tip (V_{write}) and measured the tunnel resistance (R) at low d.c. voltage ($|V_{read}| \ll |V_C|$). Figure 2c presents typical R versus V_{write} characteristics

[1]Unité Mixte de Physique CNRS/Thales, 1 Av. A. Fresnel, Campus de l'Ecole Polytechnique, 91767 Palaiseau and Université Paris-Sud, 91405 Orsay, France, [2]Université d'Evry-Val d'Essonne, Bd. F. Mitterrand, 91025 Evry, France, [3]Department of Materials Science, University of Cambridge, Cambridge CB2 3QZ, UK, [4]Thales Research and Technology, 1 Av. A. Fresnel, Campus de l'Ecole Polytechnique, 91767 Palaiseau, France, [5]Asylum Research, 6310 Hollister Avenue, Santa Barbara, California 93117, USA. *e-mail: vincent.garcia@thalesgroup.com

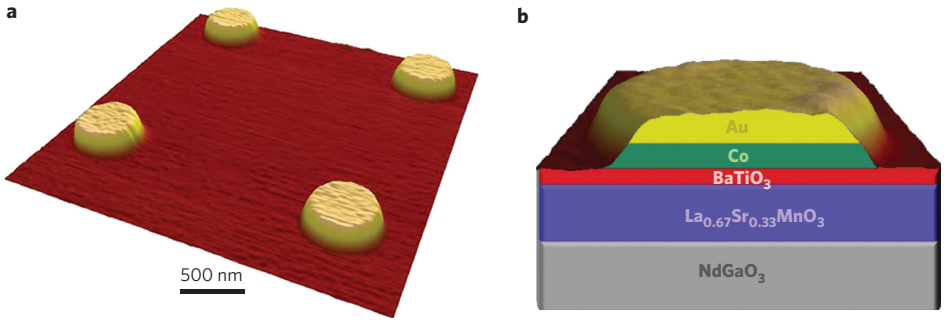

Figure 1 | Sketch of the devices. a, AFM image of four typical nanodevices defined using electron-beam lithography. **b**, Schematic of one gold/cobalt/BTO/LSMO nanodevice on a NGO substrate.

measured at $V_{read} = 100$ mV after applying successive values of V_{write} from −3.5 to +3 V and from +3 to −3.5 V. A clear large hysteretic variation of the resistance state with V_{write} is observed,

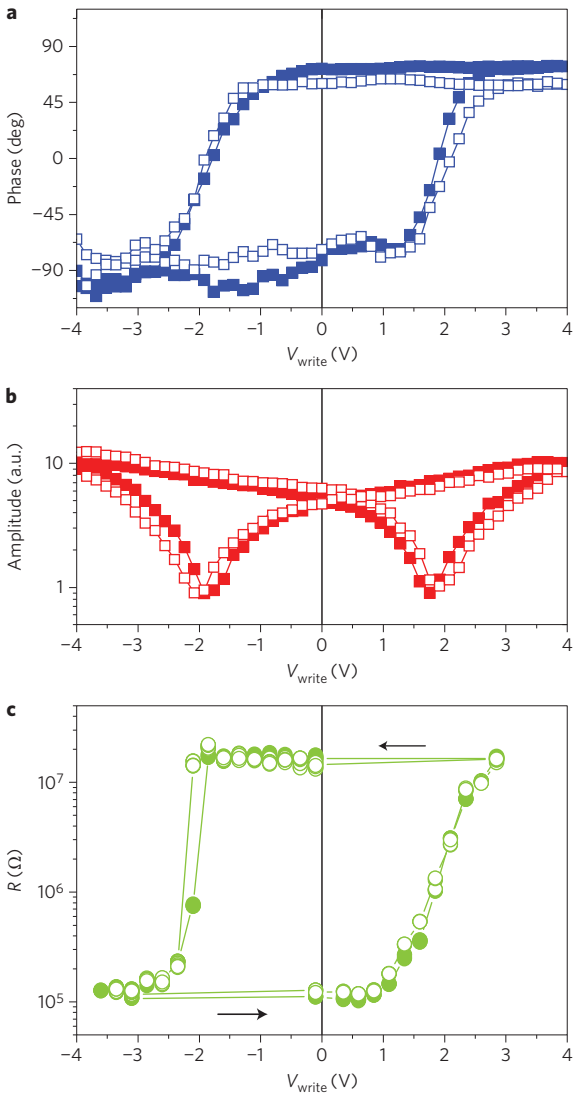

Figure 2 | Ferroelectric switching versus resistive switching. a,**b**, Out-of-plane PFM phase (**a**) and amplitude (**b**) measurements on a typical gold/cobalt/BTO/LSMO ferroelectric tunnel junction. **c**, $R(V_{write})$ for a similar capacitor measured in remanence ($V_{read} = 100$ mV) after applying successive voltage pulses of 100 μs. The open and filled circles represent two different scans to show reproducibility.

and well-defined resistive switching occurs at the coercive voltage inferred from the PFM loops. Following Kohlstedt *et al.*[18] and Maksymovych *et al.*[20], we argue that resistive switching is most probably due to ferroelectric polarization reversal in our junctions, although more complex resistive switching mechanisms involving electrochemical interface reactions associated with ferroelectric polarization reversal cannot be completely excluded[24,25]. At positive V_C, resistance switches from a low to a high value and the device is in the high resistance ('OFF') state when the polarization is pointing towards the LSMO. Symmetrically, the low resistance ('ON') state is reached by orienting the polarization towards the cobalt.

We then applied voltage pulses larger than the coercive field ($|V_{write}| > |V_C|$) and characterized the ON and OFF states in more detail. Note that the poling (or 'write') operation requires a write power of $\sim 1 \times 10^4$ A cm^{-2}. This is at least two orders of magnitude lower than the value required for MRAMs (ref. 2). Figure 3a presents a series of junction readout operations at $V_{read} = 100$ mV for the ON and OFF states, which have resistances of $\sim 1 \times 10^5$ and 1×10^7 Ω, respectively. This corresponds to a TER effect of 10,000% or an OFF/ON ratio of 100. This number agrees well with the value measured across 2-nm-thick BTO barriers by CTAFM on pre-poled ferroelectric domains[19]. It is larger than what we have found at low temperatures in iron/BTO/LSMO junctions with 1-nm-thick BTO barriers[26], which we interpret as being a result of the larger barrier thickness and the more effective poling procedure that we have used here (Supplementary Information). From Fig. 3a it is clear that both states are very stable for successive readouts.

Figure 3b shows $I(V_{read})$ between −0.5 and 0.5 V in the ON and OFF states. Both are nonlinear, highly symmetric and free of discontinuities, in contrast with what often occurs with other resistive switching devices[6]. Both traces can be well fitted using classical models of direct quantum-mechanical tunnelling through trapezoidal tunnel barriers[21,27] (Supplementary Fig. S1), indicating that mechanisms based on the modulation of tunnel transmission (through variation of the barrier height and the tunnelling effective mass) by ferroelectricity are probably responsible for the TER effect[10,11]. Additional $I(V_{read})$ measurements collected at 85 K for the ON and OFF states (Fig. 3c) show little variations from those obtained at room temperature (the current drops by less than a factor of 3 in the ON or OFF states, and the OFF/ON ratio is ∼100 at 85 K). This confirms that transport occurs by direct quantum-mechanical tunnelling through the ultrathin BTO films. Furthermore, the relative difference in the current level in the OFF and ON states and the TER do not decrease rapidly with V_{read} (Fig. 3d), allowing the readout levels to be increased with limited performance loss.

Figure 4a shows the ON and OFF resistance states for 50 junctions with an average OFF/ON ratio of 64. The reproducibility of both resistance levels and the TER effect attest to the high yield and good uniformity of the sample. The ON and OFF states are

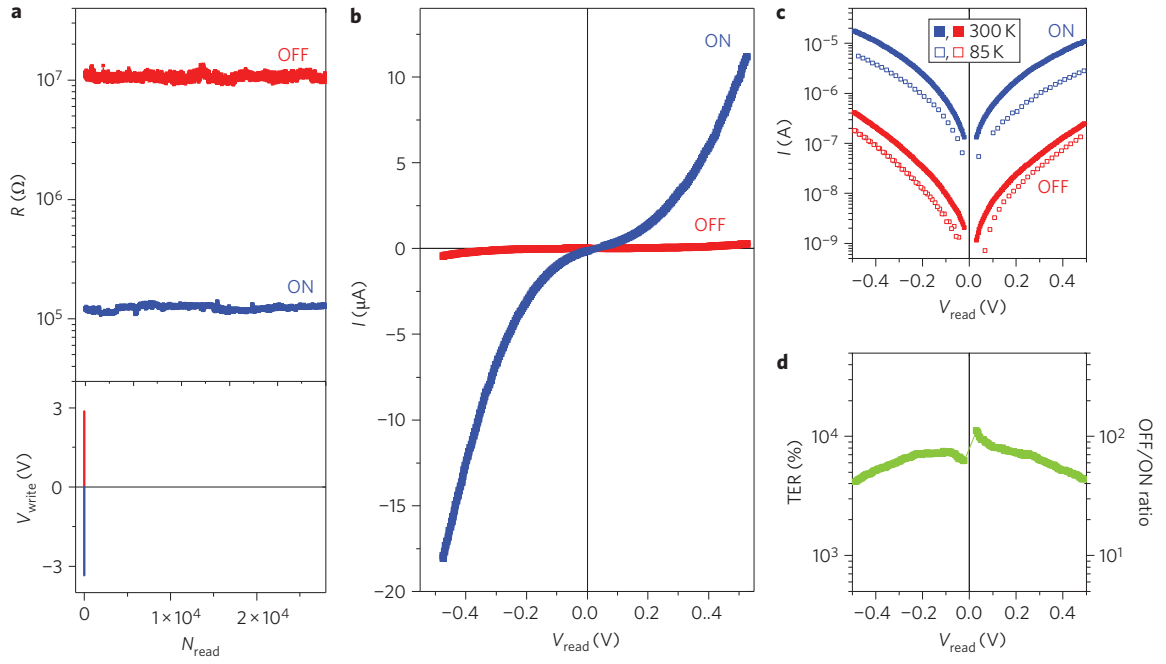

Figure 3 | Direct tunnelling with large OFF/ON ratio. a, Resistance versus time of a typical device measured at $V_{read} = 100$ mV after applying a 100 μs voltage pulse of +2.9 V (−3.4 V) to set the OFF (ON) state. **b**, $I(V_{read})$ for the same device in the ON and OFF states. **c**, Same $|I|(V_{read})$ in log scale (filled circles) with additional $I(V_{read})$ collected in the ON and OFF states at 85 K (open circles). **d**, TER(V_{read}) calculated from $I(V_{read})$.

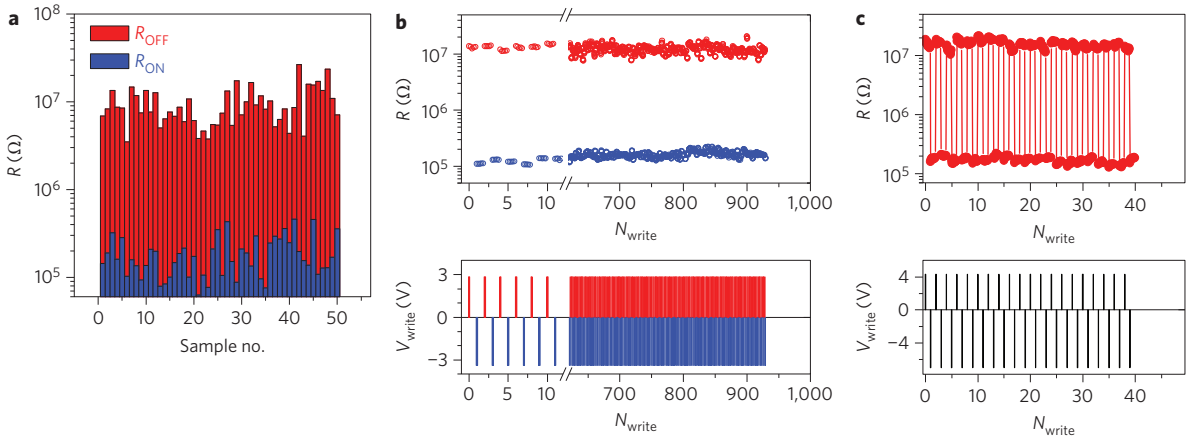

Figure 4 | Reproducible, fast and reversible switching. a, ON and OFF resistance states measured after applying 100 μs voltage pulses to 50 different junctions. Average OFF/ON ratio is 64 (range, 15–220). **b**, Reversible resistance switching between ON and OFF resistance states of a typical junction for more than 900 cycles (five resistance measurements are carried out at $V_{read} = 100$ mV between each 100 μs voltage pulse of +2.9 V and −3.4 V). **c**, OFF/ON resistance switching of a typical device measured at $V_{read} = 100$ mV after applying 10 ns voltage pulses.

highly stable over read/write cycles and do not exhibit resistance variations related to fatigue. Fatigue tests were performed over 900 read/write cycles (Fig. 4b), after which electrical contact was lost due to tip drift. The device displayed the same ON and OFF resistance states after repositioning the tip. Fully patterned junctions with permanent electric contacts should allow further endurance characterization and investigation of TER dynamics up to the gigahertz range. Complementary experiments were performed to show resistive switching in FTJs with high OFF/ON ratio (>100) after applying write voltage pulses of 10 ns (Fig. 4c). We calculated write energies of ∼100 fJ/bit for these devices (Supplementary Information). Additionally, preliminary experiments with 50-nm-wide nanojunctions (Supplementary Fig. S2) suggest ultimate write energies <10 fJ/bit, which is competitive with other non-volatile memory technologies (Supplementary Table 1)[28].

Although all the above results have been obtained on non-fully optimized devices, they constitute a proof of concept for novel types of memories based on nanoscale ferroelectrics. The electrostatic mechanism probably responsible for the TER effect strongly depends on the screening lengths at both barrier/electrode interfaces and on the barrier characteristics (dielectric constant and polarization)[10]. Strain engineering[22] and a careful control of electrical boundary conditions[29] are valuable means with which to adjust these parameters and achieve enhanced performance.

As well as their potential as non-volatile memories, solid-state FTJs also demonstrate exciting perspectives at a basic science level. Combining epitaxial electrodes and ferroelectric barrier systems would enable investigations of the interplay between ferroelectric polarization reversal and the symmetry of tunnelling wavefunctions[8]. FTJ coupling with magnetic electrodes has the potential

to yield low-power electric-field-controllable spintronics device operation at room temperature. Furthermore, FTJs are emerging as ideal systems with which to investigate polarization switching mechanisms[30] and high-frequency dynamics of nanoscale ferroelectrics, a virtually unexplored area.

Methods

The BTO/LSMO bilayers were grown on (001)$NdGaO_3$ single-crystal substrates by means of pulsed laser deposition (KrF excimer laser ($\lambda = 248$ nm), fluence of 2 J cm^{-2}, repetition rate of 1 Hz). LSMO films (30 nm) were grown at 775 °C under 0.15 mbar oxygen. BTO films were subsequently grown at 775 °C and 0.10 mbar oxygen. The samples were annealed for 1 h at 750 °C and 500 mbar oxygen and cooled to room temperature at 10 °C min^{-1}. The thickness of the films was calibrated with X-ray reflectivity and cross-checked with transmission electron microscopy[19]. Nanodevices with diameters ranging from 200 to 700 nm were defined from these bilayers using electron-beam lithography and lift-off of sputter-deposited cobalt (10 nm) followed by a capping layer of gold (10 nm). PFM experiments were performed at room temperature using a MFP-3D Asylum AFM in DART (dual a.c. resonance tracking)[31] mode. Commercial silicon tips coated with chromium/platinum (Budget Sensors) were used for PFM at typical contact resonance frequencies of 1.2–1.3 MHz. Electrical measurements were performed either with the MFP-3D or with a multimode Nanoscope IV set-up (Digital Instruments) at room temperature and under nitrogen flow with the same AFM tips. Additional low-temperature (85 K) experiments were performed using an AttoAFM I (Attocube Systems) and commercial silicon tips coated with boron-doped diamond (Nanosensors). The bias voltage was applied to the tip, and the sample was grounded for all measurements.

Received 15 September 2011; accepted 2 November 2011; published online 4 December 2011

References

1. Schmid, H. Some symmetry aspects of ferroics and single phase multiferroics. *J. Phys. Condens. Matter* **20,** 434201 (2008).
2. Ikeda, S. *et al.* Magnetic tunnel junctions for spintronic memories and beyond. *IEEE Trans. Electron. Dev.* **54,** 991–1002 (2007).
3. Moodera, J. S., Kinder, L. R., Wong, T. M. & Meservey, R. Large magnetoresistance at room temperature in ferromagnetic thin film tunnel junctions. *Phys. Rev. Lett.* **74,** 3273–3276 (1995).
4. Waser, R. & Aono, M. Nanoionics-based resistive switching memories. *Nature Mater.* **6,** 833–840 (2007).
5. Yang, J. J. *et al.* Memristive switching mechanisms for metal/oxide/metal nanodevices. *Nature Nanotech.* **3,** 429–433 (2008).
6. Jo, S. H., Kim, K-H. & Lu, W. High-density crossbar arrays based on a Si memristive system. *Nano Lett.* **9,** 870–874 (2009).
7. Dawber, M., Rabe, K. M. & Scott, J. F. Physics of thin-film ferroelectric oxides. *Rev. Mod. Phys.* **77,** 1083–1130 (2005).
8. Velev, J. P. *et al.* Magnetic tunnel junctions with ferroelectric barriers: predictions of four resistance states from first principles. *Nano Lett.* **9,** 427–432 (2009).
9. Tsymbal, E. Y. & Kohlstedt, H. Tunneling across a ferroelectric. *Science* **313,** 181–183 (2006).
10. Zhuravlev, M. Y., Sabirianov, R. F., Jaswal, S. S. & Tsymbal, E. Y. Giant electroresistance in ferroelectric tunnel junctions. *Phys. Rev. Lett.* **94,** 246802 (2005).
11. Kohlstedt, H., Pertsev, N. A., Rodriguez Contreras, J. & Waser, R. Theoretical current–voltage characteristics of ferroelectric tunnel junctions. *Phys. Rev. B* **72,** 125341 (2005).
12. Esaki, L., Laibowitz, R. B. & Stiles, P. J. Polar switch. *IBM Tech. Discl. Bull.* **13,** 2161 (1971).
13. Tybell, T., Ahn, C. H. & Triscone, J-M. Ferroelectricity in thin perovskite films. *Appl. Phys. Lett.* **75,** 856–858 (1999).
14. Junquera, J. & Ghosez, P. Critical thickness for ferroelectricity in perovskite ultrathin films. *Nature* **422,** 506–509 (2003).
15. Fong, D. D. *et al.* Ferroelectricity in ultrathin perovskite films. *Science* **304,** 1650–1653 (2004).
16. Kim, Y. S. *et al.* Critical thickness of ultrathin ferroelectric $BaTiO_3$ films. *Appl. Phys. Lett.* **86,** 102907 (2005).
17. Rodriguez-Contreras, J. *et al.* Resistive switching in metal–ferroelectric–metal junctions. *Appl. Phys. Lett.* **83,** 4595–4597 (2003).
18. Kohlstedt, H. *et al.* Method to distinguish ferroelectric from nonferroelectric origin in case of resistive switching in ferroelectric capacitors. *Appl. Phys. Lett.* **92,** 062907 (2008).
19. Garcia, V. *et al.* Giant tunnel electroresistance for non-destructive readout of ferroelectric states. *Nature* **460,** 81–84 (2009).
20. Maksymovych, P. *et al.* Polarisation control of electron tunneling into ferroelectric surfaces. *Science* **324,** 1421–1425 (2009).
21. Gruverman, A. *et al.* Tunneling electroresistance effect in ferroelectric tunnel junctions at the nanoscale. *Nano Lett.* **9,** 3539–3543 (2009).
22. Choi, K. J. *et al.* Enhancement of ferroelectricity in strained $BaTiO_3$ thin films. *Science* **306,** 1005–1009 (2004).
23. Kalinin, S. V. *et al.* The role of electrochemical phenomena in scanning probe microscopy of ferroelectric thin films. *ACS Nano* **26,** 5683–5691 (2001).
24. Wang, R. V. *et al.* Reversible chemical switching of a ferroelectric film. *Phys. Rev. Lett.* **102,** 047601 (2009).
25. Bristowe, N. C. *et al.* Electrochemical ferroelectric switching. Preprint at http://arXiv.org/1108.2208 (2011).
26. Garcia, V. *et al.* Ferroelectric control of spin polarisation. *Science* **327,** 1106–1110 (2010).
27. Brinkman, W. F., Dynes, R. C. & Rowell, J. M. Tunneling conductance of asymmetrical barriers. *J. Appl. Phys.* **41,** 1915–1921 (1970).
28. International Technology Roadmap for Semiconductors, 2009; available at http://www.itrs.net/links/2009itrs/home2009.htm.
29. Stengel, M., Vanderbilt, D. & Spaldin, N. A. Enhancement of ferroelectricity at metal–oxide interfaces. *Nature Mater.* **8,** 392–397 (2009).
30. Highland, M. J. *et al.* Polarisation switching without domain formation at the intrinsic coercive field in ultrathin ferroelectric $PbTiO_3$. *Phys. Rev. Lett.* **105,** 167601 (2010).
31. Rodriguez, B. J., Callahan, C., Kalinin, S. V. & Proksch, R. Dual-frequency resonance-tracking atomic force microscopy. *Nanotechnology* **18,** 475504 (2007).

Acknowledgements

The authors thank H. Jaffrès, P. Seneor and P. Metaxas for fruitful discussions as well as S. Vinzelberg, R. Goschke and B. Holmes at Atomic Force for technical assistance with the PFM measurements. Financial support from the European Research Council (ERC advanced grant no. 267579), French C-Nano Île de France and the French Réseau Thématique de Recherche Avancée Triangle de la Physique is acknowledged. X.M. acknowledges support from the Herchel Smith Fellowship.

Author contributions

V.G., K.B., M.B. and A.B. conceived and designed the experiments. X.M., N.D.M., A.Cr., J.A., S.X., B.D. and C.D. were responsible for the preparation and nanofabrication of the samples. A.Ch., V.G., K.B., S.F., A.M. and R.P. performed the PFM measurements. A.Ch., A.Cr., V.G., J.G., K.B. and S.F. performed the electrical measurements. A.Ch., A.Cr., V.G., S.F., K.B., M.B. and A.B. analyzed the data. V.G. and M.B. co-wrote the paper. All authors contributed to the manuscript and the interpretation of the data.

Additional information

The authors declare no competing financial interests. Supplementary information accompanies this paper at www.nature.com/naturenanotechnology. Reprints and permission information is available online at http://www.nature.com/reprints. Correspondence and requests for materials should be addressed to V.G.